Journal of Zhejiang University-SCIENCE B (Biomedicine & Biotechnology) *2021 22(9):746-756*
www.jzus.zju.edu.cn; www.springer.com/journal/11585
E-mail: jzus_b@zju.edu.cn

Research Article

https://doi.org/10.1631/jzus.B2100053

Endoplasmic reticulum stress is involved in retinal injury induced by repeated transient spikes of intraocular pressure

Xue YANG[1], Xiaowei YU[1], Zhenni ZHAO[1], Yuqing HE[1], Jiamin ZHANG[1], Xiaoqian SU[1], Nannan SUN[1]✉, Zhigang FAN[1,2]✉

[1]*State Key Laboratory of Ophthalmology, Department of Glaucoma, Zhongshan Ophthalmic Center, Sun Yat-sen University, Guangzhou 510060, China*
[2]*Tongren Eye Center, Beijing Tongren Hospital, Capital Medical School, Beijing 100730, China*

Abstract: Clinically, a large proportion of glaucoma patients undergo repeated intraocular pressure (IOP) spike (Spike IOP) attacks during their sleep, which may facilitate retinopathy. In this study, we established a mouse model of repeated transient Spike IOP to investigate the direct damage to the retina following Spike IOP attacks, and elucidated the underlying molecular mechanism. We analyzed the changes in the number of retinal ganglion cells (RGCs) via immunofluorescence. Thereafter, we detected retinal cell apoptosis via terminal deoxynucleotidyl transferase deoxyuridine triphosphate (dUTP) nick-end labeling (TUNEL) staining, and performed RNA sequencing (RNA-seq) to reveal the underlying molecular mechanism. Finally, we validated the expression of key molecules in the endoplasmic reticulum (ER) stress pathway using quantitative real-time polymerase chain reaction (qRT-PCR) and western blot analysis. Results revealed a time-dependent RGC loss in Spike IOP, evidenced by a reduction in the number of Brn3a-positive RGCs in experimental eyes following a 7-d continuous treatment with Spike IOP. In addition, TUNEL staining indicated that apoptosis of retinal cells started in the outer nuclear layer (ONL), and then spread to the ganglion cell layer (GCL) with time. RNA-seq analysis revealed that ER stress might be involved in Spike IOP-induced retinal injury. This result was corroborated by western blot, which revealed upregulation of ER stress-related proteins including binding immunoglobulin protein/glucose-regulated protein 78 (BiP/GRP78), phosphorylated inositol-requiring enzyme 1 (p-IRE1), unspliced X-box-binding protein 1 (XBP1-u), spliced X-box-binding protein 1 (XBP1-s), phosphorylated c-Jun N-terminal kinase (p-JNK), C/EBP-homologous protein (CHOP), and B-cell lymphoma 2 (Bcl-2)-associated X protein (Bax). These findings indicate that repeated IOP transients are detrimental to the retina, while ER stress plays an important role in retinal cell apoptosis in this situation. Notably, repeated Spike IOP among glaucoma patients is a crucial factor for progressive retinopathy.

Key words: Endoplasmic reticulum (ER) stress; Intraocular pressure spike (Spike IOP); Retinal injury; Neuron apoptosis; Glaucoma

1 Introduction

Glaucoma, characterized by progressive degeneration of retinal ganglion cells (RGCs) and their axons, is a major cause of irreversible vision loss worldwide. It is estimated that 111.8 million people, aged 40–80 years, will suffer from glaucoma by 2040 (Tham et al., 2014). Although the exact pathophysiology of glaucoma is not well understood, intraocular pressure (IOP) elevation has been identified as a strong risk factor for its development and progression. To date, reducing IOP either by medication or surgery is the only proven approach for slowing progression of optic neuropathy (Weinreb et al., 2014). Therefore, IOP monitoring represents a significant strategy for reducing pathologically high IOP to the desired level.

Currently, IOP profiles of patients with glaucoma are obtained from spot measurements during clinical visits within office hours. However, most patients present with normal or close to normal IOP during this period. Data from several IOP measurements within a 24-h period showed that approximately two thirds of all glaucoma patients exhibited Spike IOP

✉ Zhigang FAN, fanzhigang@mail.ccmu.edu.cn
Nannan SUN, sun_nann@163.com
Zhigang FAN, https://orcid.org/0000-0002-1190-0894
Nannan SUN, https://orcid.org/0000-0002-8810-0078

Received Jan. 24, 2021; Revision accepted Apr. 13, 2021; Crosschecked July 14, 2021

outside regular office time, and this most frequently happened during the nocturnal or sleep period (Barkana et al., 2006). Repeated occurrences of peak IOP within a short time, or fluctuations in IOP which cannot be captured by a static measurement method, may contribute to retinal injury (Asrani et al., 2000; Nouri-Mahdavi et al., 2004; Konstas et al., 2012). In the present study, we specifically established a mouse model that received a sequence of transient moderate increments in IOP (50 mmHg; 1 mmHg=0.133 kPa) to simulate occurrence of repeated Spike IOP attacks during sleep time in glaucoma patients. We used this model to investigate the effects of this change in IOP on the retina.

2 Materials and methods

2.1 Animals

Adult male C57BL/6 mice (eight weeks old; wild type (WT)) were purchased from the Model Animal Research Center of Nanjing University (China). The animals were kept under a 12-h light/dark cycle at constant temperature (26 ℃), with food and water available ad libitum. All animal experiments were conducted in adherence to the Association for Research in Vision and Ophthalmology (ARVO) Statement for Use of Animals in Ophthalmic and Visual Research, with approval from the Animal Ethics Committee of Zhongshan Ophthalmic Center of Sun Yat-sen University, Guangzhou, China.

2.2 Establishment of a Spike IOP mouse model

Mice were first anesthetized by intraperitoneal injection with 1% (0.01 g/mL) sodium pentobarbital (0.01 mL/g). Eyes were fully dilated bilaterally using 1% (0.01 g/mL) tropicamide and topically anesthetized with 0.5% (5 g/L) tetracaine hydrochloride. Then a 32-gauge needle connected to a column of saline (0.9% (9 g/L) NaCl) was inserted into the anterior chamber of the right eye, as previously described (Zhao et al., 2020). The peak IOP value was set at 50 mmHg by positioning the column at the appropriate height. According to the following equation (at standard atmospheric pressure): pressure (mmHg)=column height (cm)×10/13.6 (with a mercury density of 13.6 g/cm^3 and water density of 1 g/cm^3), 50 mmHg is equivalent to a column with a 68-cm water height. For Spike IOP, the mice's eyes were rapidly increased to 50 mmHg for 1 min by infusing saline, and then the infusion was cut off with forceps for 1 min. This operation was consistently repeated seven times. Control eyes were operated in the same way, without a pressure increase. Antibiotic eye ointment was used postoperatively to prevent infection. Mice were treated with Spike IOP for 1, 3, and 7 d. After 1 d of Spike IOP induction, four mice were randomly selected for whole-mount retinas and three for terminal deoxynucleotidyl transferase deoxyuridine triphosphate (dUTP) nick-end labeling (TUNEL) assay. We applied a similar design in mice that underwent 3 d of Spike IOP induction. For mice undergoing a seven-consecutive-day induction, two, four, three, six, and six were randomly selected for RNA sequencing (RNA-seq), whole-mount retinas, TUNEL assay, quantitative real-time polymerase chain reaction (qRT-PCR), and western blot analyses, respectively.

2.3 Tissue preparation and immunofluorescence of whole-mount retinas

Mice were anesthetized using an overdose of sodium pentobarbital, and then subjected to intracardiac perfusion with ice-cold phosphate-buffered saline (PBS) followed by 4% (volume fraction) paraformaldehyde (PFA). Four mice were used for whole-mount retinas and three for frozen retinal sections. Their eyes were enucleated and immersed into 4% PFA for another 2 h at room temperature. For frozen retinal sections, anterior segments were removed, and the eyes were dehydrated overnight in 30% (0.30 g/mL) sucrose solutions at 4 ℃. Eye cups were frozen at −80 ℃ after being embedded in optimal cutting temperature compound (Sakura, Torrance, CA, USA). Frozen sections (15 μm; through the optic nerve head) were obtained and stored at −20 ℃. For whole mounts, the retinas were isolated from eye cups and dissected by four radial incisions. Frozen sections and whole-mount retinas were prepared after 1-, 3-, and 7-d of Spike IOP treatment.

The retinas were first incubated in a blocking solution containing 0.5% (volume fraction) Triton X-100 and 5% (0.05 g/mL) bovine serum albumin (BSA) for 2 h at room temperature, and then with a mouse polyclonal anti-Brn3a (1∶50 (volume ratio; the same below); ABN1376; Merck, USA) at 4 ℃ overnight. The samples were rinsed three times with 0.01 mol/L PBS, and then incubated with a secondary antibody, donkey

anti-mouse Alexa Fluor 488 (1:800; A21202; Invitrogen, USA), for 2 h at room temperature. Cell nuclei were counterstained with 4',6-diamidino-2-phenylindole (DAPI; Sigma Aldrich, St. Loius, MO, USA) for 5 min, washed three times, and then mounted on glass slides with the ganglion cell layer (GCL) facing up. The slides were cover-slipped using 70% (volume fraction) glycerin, and images were acquired using a fluorescence microscope (DMI 8, Leica, Germany). To quantify immuno-positive RGCs, each retina was divided into central, middle, and peripheral areas, at distances of 1, 2, and 3 mm from the optic disc, respectively; then three areas in each quadrant (total 12) were selected for counting under a 40× objective lens (311 μm× 233 μm microscope fields). Finally, we calculated the average number of Brn3a-positive cells per mm^2. Quantification was performed by two investigators in a blinded manner.

2.4 TUNEL assay

We obtained frozen retinal sections from another three mice at each time point, and stained them using a TUNEL kit (Vazyme Biotech Co., Ltd., China) according to the manufacturer's instructions, to detect retinal neuronal apoptosis. Briefly, tissue sections were re-hydrated in 4% PFA at room temperature for 30 min and penetrated with proteinase K for 10 min. The sections were incubated in equilibration buffer for 20 min, and then with a TUNEL reaction mixture at 37 °C for 1 h in a humidified and dark chamber. Finally, we examined the sections under a fluorescence microscope (DMI 8, Leica), and two observers counted the number of TUNEL-positive cells in the whole section in a blinded manner. Twelve sections (six from control eyes and six from experimental eyes) from three mice were used for TUNEL study at each time point.

2.5 RNA-seq analysis

We isolated total RNA of each retina from two control eyes and two experimental eyes, and purified it using the TRIzol reagent (Invitrogen, Carlsbad, CA, USA) according to the manufacturer's instructions. The RNA was quantified and used to construct libraries using the TruSeq® Stranded Total RNA LT Library Prep Kit (Illumina, USA) following the manufacturer's instructions. The complementary DNA (cDNA) libraries (average insert size of (300±50) bp) were sequenced on an Illumina Novaseq™ 6000 platform (LC-Bio Technology Co., Ltd., Hangzhou, China) according to the vendor's recommended protocol, to generate 2× 150 bp paired-end reads (PE150).

We removed adaptors from the reads using Cutadapt software (Version cutadapt-1.9; https://cutadapt.readthedocs.io/en/stable/guide.html), and then trimmed low-quality bases; the next step involved mapping the resulting clean reads onto a reference genome using HISAT2 software (Version hisat2-2.0.4; http://daehwankimlab.github.io/hisat2). Mapped reads for each sample were assembled using StringTie (Version stringtie-1.3.4d.Linux_x86_64; http://ccb.jhu.edu/software/stringtie/index.shtml?t=manual), with default parameters; then all transcriptomes from all samples were merged using gffcompare software (Version gffcompare-0.9.8. Linux_x86_64; http://ccb.jhu.edu/software/stringtie/gffcompare.shtml) to reconstruct a comprehensive transcriptome. Finally, we estimated expression levels for all transcripts using StringTie and Ballgown, and we analyzed expression levels for messenger RNAs (mRNAs) by calculating fragments per kilobase of exon model per million mapped reads (FPKM). Differential gene expression analysis was performed using R package edgeR or DESeq2, and then gene ontology (GO) and Kyoto encyclopedia of genes and genomes (KEGG) enrichment analyses were performed to reveal gene function.

2.6 qRT-PCR

We validated the expression of key molecules in the endoplasmic reticulum (ER) stress pathway using qRT-PCR. Briefly, retinas were individually collected from six mice (six control eyes and six experimental eyes) after 7 d of Spike IOP induction, and their total RNAs were extracted using TRIzol reagent (Invitrogen). The RNA was quantified, and then reverse-transcribed to cDNA using the First-Strand cDNA Synthesis Kit (Applied Biological Materials (ABM) Inc., Richmond, BC, Canada) according to the manufacturer's instructions. We performed qRT-PCR on the cDNA in a Roche LightCycler 384 system, using SYBR Green Master Mix (Roche Life Science, Basel, Switzerland). We evaluated the threshold cycle of fluorescence units to quantify the amount of each mRNA level and used β-actin as the endogenous amplification control. Primer sequences for the target genes are listed in Table S1.

2.7 Western blot analysis

Control and experimentally treated eyes from six mice were enucleated after 7 d of Spike IOP induction, and their retinas were immediately frozen in liquid nitrogen after dissection. To extract proteins, each sample was lysed in 100 μL ice-cold radioimmunoprecipitation assay (RIPA) buffer (Fd Bioscience, Hangzhou, China) supplemented with protease inhibitors and sonicated. The homogenates were centrifuged at 12 000*g* at 4 ℃ for 5 min, and the supernatants were collected and mixed with 6× loading buffer (Fd Boscience). Proteins were denatured at 95 ℃ for 5 min, separated on a 12% (0.12 g/mL) sodium dodecyl sulfate-polyacrylamide gel electrophoresis (SDS-PAGE), and then electroblotted onto polyvinylidene fluoride membranes (Millipore, Bedford, MA, USA). The membranes were blocked with 5% (0.05 g/mL) skim milk at room temperature for 2 h, and then incubated overnight at 4 ℃ with the following primary antibodies: anti-binding immunoglobulin protein/glucose-regulated protein 78 (anti-BiP/GRP78) antibody (1: 2000 (volume ratio; the same below); Signalway Antibody, MD, USA), anti-phosphorylated inositol requiring enzyme 1 (anti-p-IRE1) antibody (1: 2000; Signalway Antibody), anti-X-box-binding protein 1 (anti-XBP1) antibody (1:1000; Proteintech, Wuhan, China), anti-C/EBP-homologous protein (anti-CHOP) antibody (1:1000; Signalway Antibody), anti-B-cell lymphoma-2 (anti-Bcl-2) antibody (1:500; Proteintech), anti-Bcl-2-associated X protein (anti-Bax) antibody (1: 500; Proteintech), anti-c-Jun N-terminal kinase (anti-JNK) antibody (1:1000; Signalway Antibody), and anti-phosphorylated c-Jun N-terminal kinase (anti-p-JNK, Thr183/Tyr185) antibody (1:1000; Signalway Antibody). The membranes were washed three times with Tris-buffered saline with Tween 20 (TBST) (10 min for each wash), and then incubated with goat anti-mouse horse radish peroxidase (HRP)-conjugated (1:5000; Thermo, Carlsbad, CA, USA) or goat anti-rabbit HRP-conjugated secondary antibody (1:5000; Thermo) at room temperature for 2 h. The membranes were washed three times with TBST, and then scanned on an MP ChemiDoc Imaging System (Bio-Rad Laboratories, Inc., Berkeley, CA, USA). Densitometric values of the resulting western blot bands were analyzed using ImageJ software (Version 1.52a; the National Institutes of Health, USA).

2.8 Statistical analysis

Data were expressed as mean±standard error of the mean (SEM). We compared the two groups with a Student's *t*-test, implemented in SPSS software (Version 21.0; Chicago, IL, USA), with $P \leqslant 0.05$ considered statistically significant. We generated graphs using GraphPad Prism 8 (Version 8.0.1; La Jolla, USA).

3 Results

3.1 Time-dependent RGC loss with Spike IOP treatment

A single acute and significant increase in IOP within a short time, or even a few minutes, results in RGC loss, whereas a short-time and moderate IOP elevation may not be sufficient to cause RGC apoptosis. To determine whether repeated attacks of intermittent moderate IOP elevation can cause RGC loss, we established a Spike IOP mouse model, and then analyzed the number of RGCs using immunostaining for whole-mount retinas with the RGC-specific marker Brn3a (Fig. 1a) . Our results revealed loss of RGCs in a time-dependent manner in eyes treated with Spike IOP. Representative images showed no evidence of a reduction in density of $Brn3a^+$ RGCs in experimental eyes following Spike IOP induction for 1 and 3 d in the central, middle, and peripheral areas compared with that in corresponding control eyes (Fig. 1b). However, we observed a significant decrease in the density of $Brn3a^+$ RGCs in the central, middle, and peripheral areas after 7 d of consecutive Spike IOP induction, relative to control eyes ($P<0.05$; Fig. 1b). These results suggested that repeated Spike IOP was detrimental to RGC survival.

3.2 Retinal cell apoptosis from the outer nuclear to the ganglion cell layer

To further examine Spike IOP's damaging effects on the retina, we performed TUNEL staining on control and experimental retinal sections. Strikingly, we first detected a few TUNEL-positive cells in the outer nuclear layer (ONL) 1 d after Spike IOP induction (Fig. 2a). TUNEL-positive cells significantly increased in retinal sections after 3 d of consecutive Spike IOP induction. These were scattered within the ONL, indicating that photoreceptor cells were the initial target

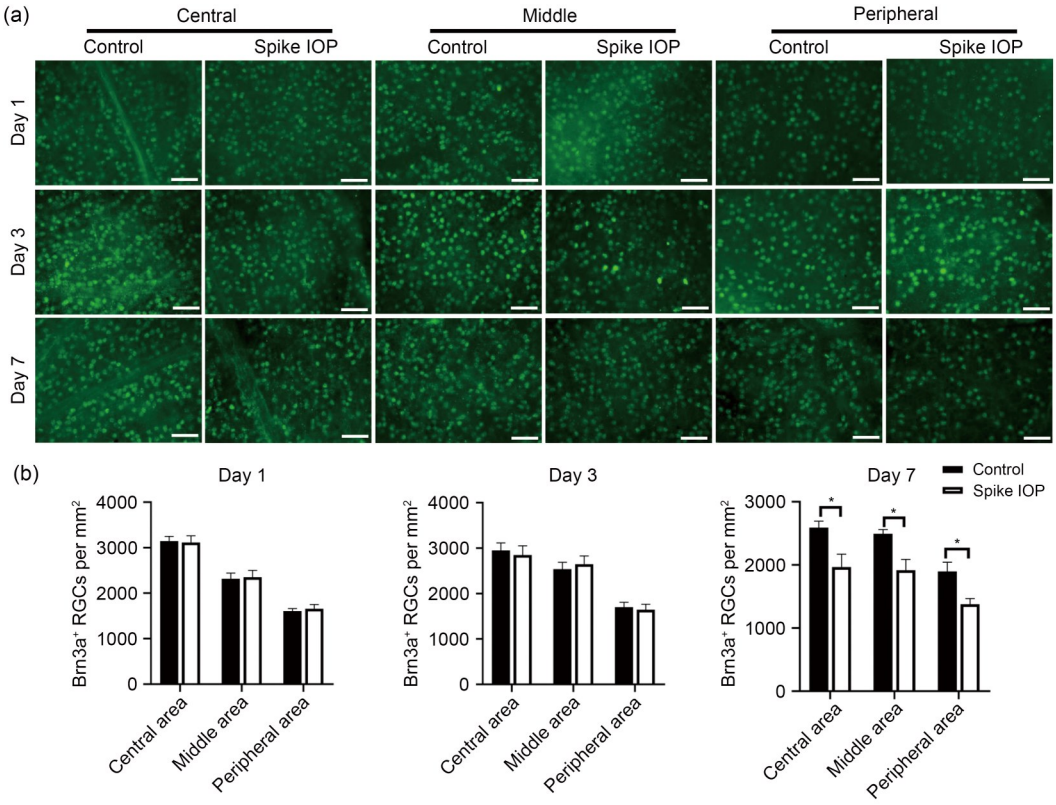

Fig. 1 Brn3a immunostaining and quantification of RGCs in a whole-mount retina from control eyes and experimental eyes after 1, 3, and 7 d of Spike IOP induction. (a) Representative images were taken from the central, middle, and peripheral areas (scale bar=50 μm). (b) RGCs in the central, middle, and peripheral areas were counted and averaged. Data are presented as mean±SEM of 16 fields per area. * P<0.05. Spike IOP: intraocular pressure (IOP) spike; RGC: retinal ganglion cell; SEM: standard error of the mean.

of damage. Seven days of consecutive Spike IOP of the eyes resulted in some apoptosis that spread inward to the inner nuclear layer (INL) (Fig. 2a). In addition, several TUNEL-positive cells emerged in the GCL (Fig. 2a), but we did not observe any in the retinal sections of control eyes. Taken together, these results indicated that Spike IOP resulted in apoptosis of various retinal neurons, which started in the ONL and then spread to the GCL as time went on. Because the retinal damage was most obvious after Spike IOP treatment for 7 d (Fig. 2b), we carried out the follow-up molecular mechanism exploration at this time point.

3.3 Effect of Spike IOP induction on ER stress in retinas

To gain insights into the underlying molecular mechanism of Spike IOP-induced retinal neuronal apoptosis, we performed whole transcriptome profiling using RNA-seq. A total of 3516 genes were differentially expressed between purified control and experimental retinas (fold change≥1.4 or ≤0.6; P≤0.05), of which 1462 and 2054 were downregulated and upregulated, respectively, in the Spike IOP-induced group. A detailed analysis of these genes revealed that most of them were associated with apoptosis and ER stress (Fig. 3a). Furthermore, GO of the differentially expressed genes revealed that they were enriched in the following biological process: "intrinsic apoptotic signaling pathway in response to endoplasmic reticulum stress" (GO: 0070059), "response to oxidative stress" (GO: 0006979), "positive regulation of mitogen-activated protein kinase (MAPK) cascade" (GO: 0043410), "apoptotic process" (GO: 0006915), and "cellular calcium ion homeostasis" (GO: 0006874), among others (Fig. 3b). These transcriptomic changes between the control and experimental groups indicated activation of the apoptosis signaling pathway and involvement of ER stress in retinal injury induced by Spike IOP.

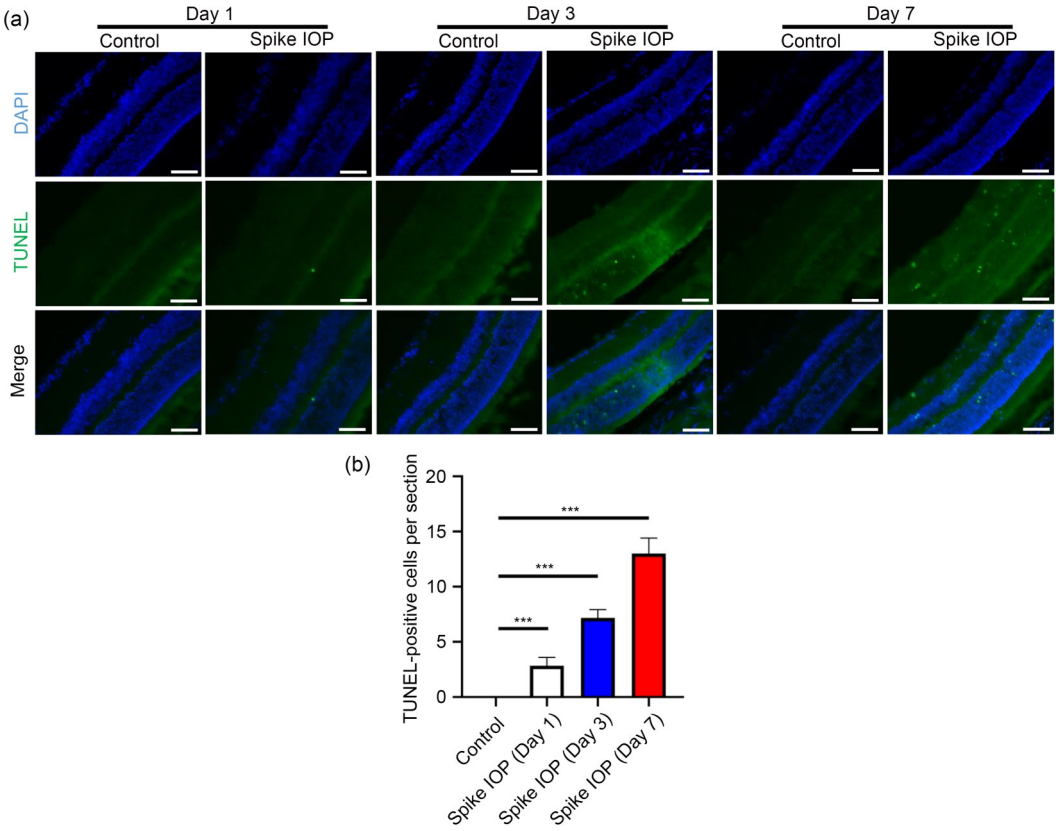

Fig. 2 TUNEL staining of retinal sections. (a) Presence of retinal neuronal apoptosis in mice in the Spike IOP group at 1, 3, and 7 d after treatment (scale bar=50 μm). (b) TUNEL-positive cells were counted and averaged in six sections from three mice per group at each time point. Data are presented as mean±SEM. *** P<0.001. DAPI: 4',6-diamidino-2-phenylindole; TUNEL: terminal deoxyuridine triphosphate (dUTP) transferase nick-end labeling; Spike IOP: intraocular pressure (IOP) spike; SEM: standard error of the mean.

3.4 Involvement of IRE1 signaling pathway in retinal neuronal apoptosis

To date, three major signaling pathways, namely the protein kinase-like ER kinase (PERK), activating transcription factor 6 (ATF6), and IRE1 pathways, have been shown to regulate ER stress (Lin et al., 2019). We used qRT-PCR to further determine the effect of Spike IOP treatment on patterns of expression of specific genes associated with the aforementioned signaling pathways. Results revealed significant upregulation of unspliced *XBP1* (*XBP1-u*; 1.69-fold) and spliced *XBP1* (*XBP1-s*; 1.79-fold) in the experimental group relative to the control group. However, we found no significant differences in the relative mRNA expression levels of *BiP*/*GRP78*, *CHOP*, or *Bax* between the two groups (Fig. 4a). Meanwhile, the anti-apoptosis gene *Bcl-2* was significantly downregulated in retinas treated with Spike IOP relative to controls (P<0.05; Fig. 4a).

We also performed western blot analysis to assess levels of protein expression across the ER stress signaling pathways. We found significant upregulation of p-IRE1, BiP/GRP78, XBP1-u, and XBP1-s in Spike IOP-treated retinas relative to control retinas (Figs. 4b and 4c). Persistent and severe ER stress caused overloaded accumulation of misfolded and unfolded proteins in ER. This overwhelmed its self-processing ability, and induced cellular apoptosis by activating the JNK, CHOP, and caspase 12 signaling pathways. Correspondingly, we found significant upregulation of p-JNK and CHOP in the experimental group compared with the control group (Fig. 4b).

4 Discussion

Peak IOP and the associated fluctuations have been proposed as major contributors to glaucoma development and progression (Zeimer et al., 1991;

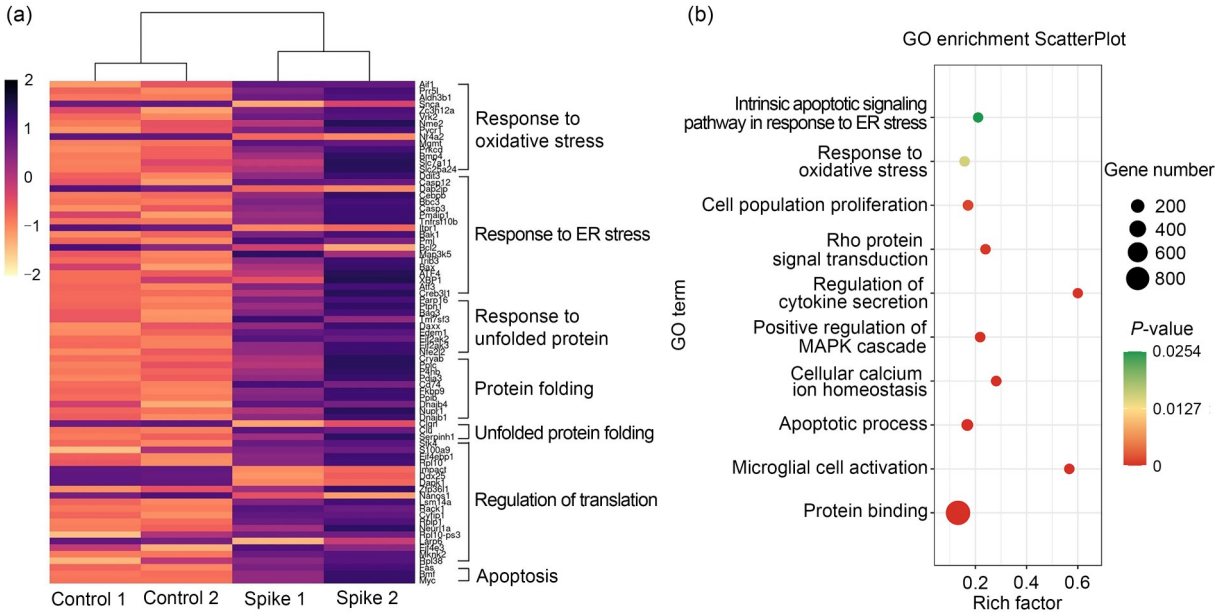

Fig. 3 RNA sequencing results. (a) Heatmap showing differentially expressed genes associated with ER stress. (b) GO showing differentially expressed genes enriched in apoptotic and other ER stress-related responses. ER: endoplasmic reticulum; GO: gene ontology; MAPK: mitogen-activated protein kinase.

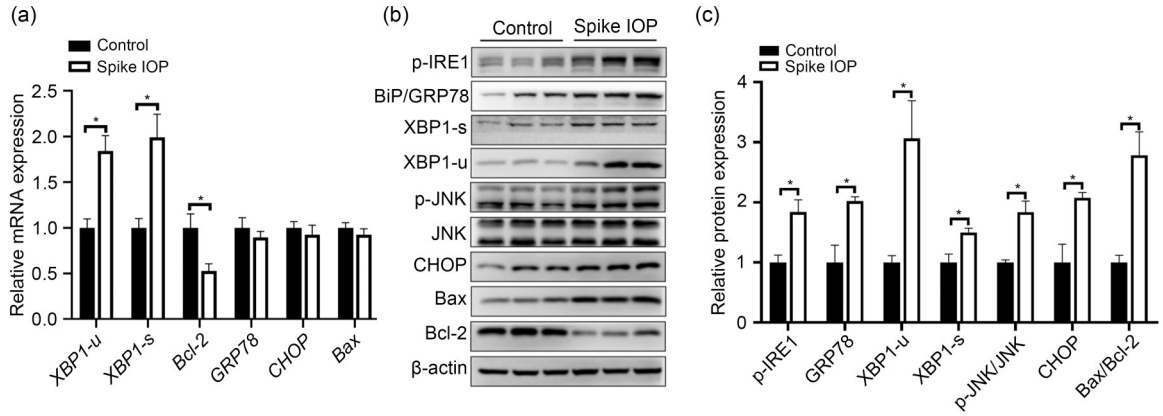

Fig. 4 Molecular markers related to ER stress in retinas of mice treated with or without Spike IOP. (a) Expression profile of different molecules in retinas quantified by qRT-PCR. β-actin was used as an endogenous amplification control. (b) Representative western blot showing changes in the expression of ER stress-related proteins. (c) Quantitative analysis of western blot of ER stress-related proteins. Data are expressed as mean±SEM (n=6). * P<0.05. Spike IOP: intraocular pressure (IOP) spike; mRNA: messenger RNA; XBP1-u: unspliced X-box-binding protein 1; XBP1-s: spliced X-box-binding protein 1; Bcl-2: B-cell lymphoma-2; GRP78: glucose-regulated protein 78; CHOP: C/EBP-homologous protein; Bax: Bcl-2-associated X protein; p-IRE1: phosphorylated inositol requiring enzyme 1; p-JNK: phosphorylated c-Jun N-terminal kinase; ER: endoplasmic reticulum; qRT-PCR: quantitative real-time polymerase chain reaction; SEM: standard error of the mean.

Konstas et al., 2012; Xu SC et al., 2016; Xu LJ et al., 2020). However, single IOP measurement in a sitting position, during routine outpatient time, does not reflect either a true spike or fluctuation of IOP throughout the day. Previous studies have shown that most patients exhibit the highest IOP levels during the nocturnal/sleep period (Liu et al., 2003, 2010), and these levels are more significant in the supine, rather than the lateral decubitus, body position. Variations in sleep-related IOP may be a potential risk for glaucoma progression, especially in patients with anxiety traits.

To mimic a situation that may happen during the sleep period in glaucoma patients, we treated mice

with a sequence of IOP spikes, and then analyzed the effects of repeated IOP spikes on the retina. Immunofluorescence of the whole retina showed a reduction in the number of RGCs after 7 d of consecutive induction. These results are consistent with RGC apoptosis detected via the TUNEL assay. Interestingly, TUNEL staining revealed the emergence of photoreceptor cell apoptosis, and this preceded RGC damage after the first day of Spike IOP induction. Moreover, apoptosis of photoreceptors became more evident after 3 and 7 d of treatment. This phenomenon has not been previously reported. Actually, loss or swelling of photoreceptors has been observed in various animal glaucoma models and in clinical glaucoma patients (Panda and Jonas, 1992; Nork et al., 2000; Choi et al., 2011; Zhao et al., 2020). Overall, our results demonstrated that repeated rapid IOP transients at 50 mmHg can cause injury to all three major retinal nuclear layers. Strikingly, it is evident that neuronal apoptosis in Spike IOP proceeds from the ONL to the GCL, which is contrary to previous findings of an acute ocular hypertension mouse model previously treated with 60 mmHg for 2 h (Zhou et al., 2019). Instead of a single increase in IOP induction, we applied a sequence of transient spikes in mice. We hypothesized that retinal neurons may have different susceptibility to distinct IOP levels. In our mouse model, we assumed that increasing IOP could directly damage retinal cells, although we cannot rule out the possibility of retinal injury occurring due to the ischemic insult.

RGC has been considered an initial damage site in glaucoma patients. Particularly, one of the potential risk factors is that in humans, the optic nerve and primary vascular vessels pass through the lamina cribrosa, where pressure may increase in response to IOP elevation, thereby disrupting retrograde transportation of brain-derived neurotrophic factors (BDNFs) and cutting off nutrition supply to the inner retina, which is followed by RGC degeneration (Hou et al., 2016; Li et al., 2020). Unlike in the human system, mice lack a lamina cribrosa, which may partially weaken the impact of IOP elevation on RGCs, although other retinal neurons may be susceptible as initial sites (May and Mittag, 2006). Photoreceptor cells convert the light falling on the retina into electrical signals, demanding a great deal of energy and oxygen, which may lower oxygen levels in the outer retina to zero (Sim and Fruttiger, 2013). However, repeated IOP transients may break the balance of a low oxygen microenvironment in the ONL, a process that is difficult to compensate for owing to the fact that the outer retina is devoid of blood vessels. This structural characteristic may predispose photoreceptors to death due to internal stress-induced activation of the inflammatory response and apoptotic signaling pathway. Similar to our findings, Ortín-Martínez et al. (2015) reported that an adult rat model of laser-photocoagulation-induced ocular hypertension showed progressive outer retinal pathology characterized by low numbers of L- and S-cone outer segments throughout the retina, which is independent of RGC loss. This may be attributed to a temporary/transient ischemia of the retina and the choroid induced by ocular hypertension that could disturb photoreceptor or pigment epithelial cell metabolism, thereby increasing the oxidative stress level (García-Ayuso et al., 2013; Wang et al., 2017). Apart from loss of photoreceptors at an early time point, we observed successive retinal cell apoptosis during later stages, which might be a secondary event. A previous study, using different animal models of inherited photoreceptor degeneration, showed that retinal remodeling following photoreceptor degeneration impaired RGC survival (Garcia-Ayuso et al., 2018). Therefore, it is rational to assume that Spike IOP-induced photoreceptor apoptosis disrupts the normal connection of the synapse, thereby causing progressive degeneration of other retinal neurons. Additionally, microglia can be simultaneously activated with initiation of photoreceptor death, with degeneration likely to be accompanied by microglial proliferation and migration to the outer retina (di Pierdomenico et al., 2017, 2019). Since neurotoxic microglia have also been implicated in causing RGC death, we hypothesized that photoreceptor apoptosis accompanied by activated microglia spreading inward to the inner retina may mediate secondary apoptosis in RGCs. However, the interaction between these cells needs further investigation.

To uncover the potential molecular mechanisms underlying retinal neuronal death, we analyzed RNA-seq data from the control and 7-d Spike IOP treatment groups and found that 3516 genes were differentially expressed between the groups. GO analysis of upregulated genes in retinas treated with Spike IOP revealed that most of them were apoptotic, whereas some were involved in ER stress-related responses. This indicated that retinal neuronal apoptosis may be partially attributed

to ER stress. Accumulating evidence has demonstrated that ER stress plays a vital role in the pathophysiology of neurodegenerative diseases, including Alzheimer's disease (AD), Parkinson's disease (PD), Huntington's disease (HD), retinitis pigmentosa, age-related macular degeneration (AMD), and glaucomatous retinopathy (Yang et al., 2007; Salminen et al., 2010; Hu et al., 2012; Kroeger et al., 2012; Hetz and Saxena, 2017). Integrating our RNA-seq evidence with previous findings affirms the role played by ER stress in loss of retinal neurons following prolonged Spike IOP treatment.

The ER is an intracellular organelle responsible for protein synthesis, proper folding, and secretion, as well as exerting essential quality control functions. Cellular stress induced by ischemia, hypoxia, and other factors has been shown to perturb ER homeostasis. This causes impaired protein assembly, followed by aggregation of unfolded and misfolded proteins (Kim et al., 2008), and triggers the unfolded protein response (UPR). Three major sensors, namely PERK, ATF6, and IRE1, have been implicated in regulation of UPR (Lin et al., 2019). UPR is a self-protective response that plays an important role in restoring ER functions. However, in case of prolonged and severe ER stress conditions, pro-apoptotic signaling pathways are initiated through regulation of CHOP, JNK, and caspase expression.

In the present study, qRT-PCR results revealed upregulation of *XBP1*, which is consistent with western blots. XBP1, a downstream transcription factor of p-IRE1, is a key molecule of the IRE1 signaling pathway. Under normal physiological (non-stressed) conditions, IRE1 interacts with BiP/GRP78 and maintains it in an inactive state. However, under ER stress, IRE1 dissociates from BiP/GRP78 and is phosphorylated into an active form (p-IRE1), which transfers XBP1-u into XBP1-s. Consequently, XBP1-s protein translocates into the nucleus, binds to the promoters of its targeted genes, and triggers UPR. Although IRE/XBP1 is thought to be protected by production of XBP1-s, the effect on neuroprotection in vivo remains unclear. Hu et al. (2012) reported that deletion of *XBP1* in RGCs caused no significant effects on RGC survival after acute traumatic injury of the optic nerve (Hu et al., 2012), while its deletion in the nervous system prolonged lifespan in an amyotrophic lateral sclerosis model (Hetz et al., 2009). Moreover, activation of IRE1 has also been shown to initiate expression of apoptotic pathways by regulating expression of JNK, as well as CHOP transcription, under severe ER stress conditions. Specifically, JNK triggers cellular apoptosis mainly by phosphorylating Bcl-2, while CHOP promotes apoptosis through downregulating Bcl-2 expression. Additionally, JNK has been shown to promote activation of pro-apoptotic protein Bax.

In our Spike IOP mouse model, upregulation of XBP1-s was accompanied by robust activation of the apoptotic signaling pathway, as evidenced by significant upregulation of p-JNK, CHOP, and Bax/Bcl-2 proteins. Overall, the pro-apoptosis effects outweigh pro-survival effects under the current Spike IOP conditions, which causes retinal neuronal death. Previous studies have demonstrated that modulating ER stress molecules, such as inhibition of JNK and CHOP, rescues retinal neurodegeneration (Sun et al., 2011; Yang et al., 2016; Kumar et al., 2019). Although our results suggested that the IRE1 signaling pathway may play an important role in retinal injury induced by Spike IOP, it is not clear whether applying interventions, such as use of an inhibitor, on key ER stress markers can alleviate neuronal apoptosis. Further studies are needed to prove this phenomenon. Nevertheless, we have successfully revealed a special damage pattern on the retina following sequential IOP spike injury, and unraveled the underlying molecular expression changes.

5 Conclusions

In summary, our results demonstrated that repeated transient IOP spikes caused retinal injury, and this was accompanied by neuronal apoptosis that spread inward from the ONL to the GCL. Analysis of transcriptomic changes revealed that ER stress is involved in loss of retinal neurons. The animal model established here has potential for exploration of detrimental effects of IOP changes and temporary/transient ischemia on the retina. Considering that a single IOP measurement cannot reflect true IOP spikes or fluctuations, a more optimal measurement approach is needed for effective clinical assessment of the risk for glaucoma progression according to IOP value. In addition, we recommend that clinicians adopt more proactive strategies when glaucoma progression is disproportionate to IOP elevation measured during regular outpatient time. Finally,

more attention should be paid to potential photoreceptor defects and impaired visual function in glaucoma patients.

Acknowledgments

This work was supported by the Guangzhou Science and Technology Plan Project (Nos. 201803040020, 201903010065, and 202102021099), the Guangdong Natural Science Foundation (No. 2020A151501168), and the Research Funds of the State Key Laboratory of Ophthalmology (No. PT1001022), China.

Author contributions

Xue YANG performed this study, collected the data, and drafted the manuscript. Zhenni ZHAO, Jiamin ZHANG, and Xiaoqian SU assisted in carrying out the research. Xiaowei YU and Yuqing HE assisted in analyzing the data. Nannan SUN and Zhigang FAN conceived the study and proofread the manuscript. All authors have read and approved the final manuscript and, therefore, have full access to all the data in the study and take responsibility for the integrity and security of the data.

Compliance with ethics guidelines

Xue YANG, Xiaowei YU, Zhenni ZHAO, Yuqing HE, Jiamin ZHANG, Xiaoqian SU, Nannan SUN, and Zhigang FAN declare that they have no conflict of interest.

All institutional and national guidelines for the care and use of laboratory animals were followed.

References

Asrani S, Zeimer R, Wilensky J, et al., 2000. Large diurnal fluctuations in intraocular pressure are an independent risk factor in patients with glaucoma. *J Glaucoma*, 9(2): 134-142.
https://doi.org/10.1097/00061198-200004000-00002

Barkana Y, Anis S, Liebmann J, et al., 2006. Clinical utility of intraocular pressure monitoring outside of normal office hours in patients with glaucoma. *Arch Ophthalmol*, 124(6): 793-797.
https://doi.org/10.1001/archopht.124.6.793

Choi SS, Zawadzki RJ, Lim MC, et al., 2011. Evidence of outer retinal changes in glaucoma patients as revealed by ultrahigh-resolution in vivo retinal imaging. *Br J Ophthalmol*, 95(1):131-141.
https://doi.org/10.1136/bjo.2010.183756

di Pierdomenico J, García-Ayuso D, Pinilla I, et al., 2017. Early events in retinal degeneration caused by rhodopsin mutation or pigment epithelium malfunction: differences and similarities. *Front Neuroanat*, 11:14.
https://doi.org/10.3389/fnana.2017.00014

di Pierdomenico J, García-Ayuso D, Agudo-Barriuso M, et al., 2019. Role of microglial cells in photoreceptor degeneration. *Neural Regen Res*, 14(7):1186-1190.
https://doi.org/10. 4103/1673-5374.251204

García-Ayuso D, Ortín-Martínez A, Jiménez-López M, et al., 2013. Changes in the photoreceptor mosaic of P23H-1 rats during retinal degeneration: implications for rod-cone dependent survival. *Invest Ophthalmol Vis Sci*, 54(8): 5888-5900.
https://doi.org/10.1167/iovs.13-12643

García-Ayuso D, di Pierdomenico J, Agudo-Barriuso M, et al., 2018. Retinal remodeling following photoreceptor degeneration causes retinal ganglion cell death. *Neural Regen Res*, 13(11):1885-1886.
https://doi.org/10.4103/1673-5374.239436

Hetz C, Saxena S, 2017. ER stress and the unfolded protein response in neurodegeneration. *Nat Rev Neurol*, 13(8): 477-491.
https://doi.org/10.1038/nrneurol.2017.99

Hetz C, Thielen P, Matus S, et al., 2009. XBP-1 deficiency in the nervous system protects against amyotrophic lateral sclerosis by increasing autophagy. *Genes Dev*, 23(19): 2294-2306.
https://doi.org/10.1101/gad.1830709

Hou RW, Zhang Z, Yang DY, et al., 2016. Pressure balance and imbalance in the optic nerve chamber: The Beijing Intracranial and Intraocular Pressure (iCOP) study. *Sci China Life Sci*, 59(5):495-503.
https://doi.org/10.1007/s11427-016-5022-9

Hu Y, Park KK, Yang L, et al., 2012. Differential effects of unfolded protein response pathways on axon injury-induced death of retinal ganglion cells. *Neuron*, 73(3):445-452.
https://doi.org/10.1016/j.neuron.2011.11.026

Kim I, Xu WJ, Reed JC, 2008. Cell death and endoplasmic reticulum stress: disease relevance and therapeutic opportunities. *Nat Rev Drug Discov*, 7(12):1013-1030.
https://doi.org/10.1038/nrd2755

Konstas AGP, Quaranta L, Mikropoulos DG, et al., 2012. Peak intraocular pressure and glaucomatous progression in primary open-angle glaucoma. *J Ocul Pharmacol Ther*, 28(1):26-32.
https://doi.org/10.1089/jop.2011.0081

Kroeger H, Messah C, Ahern K, et al., 2012. Induction of endoplasmic reticulum stress genes, *BiP* and *Chop*, in genetic and environmental models of retinal degeneration. *Invest Ophthalmol Vis Sci*, 53(12):7590-7599.
https://doi.org/10.1167/iovs.12-10221

Kumar V, Mesentier-Louro LA, Oh AJ, et al., 2019. Increased ER stress after experimental ischemic optic neuropathy and improved RGC and oligodendrocyte survival after treatment with chemical chaperon. *Invest Ophthalmol Vis Sci*, 60(6):1953-1966.
https://doi.org/10.1167/iovs.18-24890

Li J, Yang DY, Kwong JMK, et al., 2020. Long-term follow-up of optic neuropathy in chronic low cerebrospinal fluid pressure monkeys: The Beijing Intracranial and Intraocular Pressure (iCOP) study. *Sci China Life Sci*, 63(11):1762-1765.
https://doi.org/10.1007/s11427-018-1626-6

Lin T, Lee JE, Kang JW, et al., 2019. Endoplasmic reticulum (ER) stress and unfolded protein response (UPR) in mammalian oocyte maturation and preimplantation embryo development. *Int J Mol Sci*, 20(2):409.

https://doi.org/10.3390/ijms20020409

Liu JHK, Zhang XY, Kripke DF, et al., 2003. Twenty-four-hour intraocular pressure pattern associated with early glaucomatous changes. *Invest Ophthalmol Vis Sci*, 44(4):1586-1590. https://doi.org/10.1167/iovs.02-0666

Liu JHK, Medeiros FA, Slight JR, et al., 2010. Diurnal and nocturnal effects of brimonidine monotherapy on intraocular pressure. *Ophthalmology*, 117(11):2075-2079. https://doi.org/10.1016/j.ophtha.2010.03.026

May CA, Mittag T, 2006. Optic nerve degeneration in the DBA/2NNia mouse: is the lamina cribrosa important in the development of glaucomatous optic neuropathy? *Acta Neuropathol*, 111(2):158-167. https://doi.org/10.1007/s00401-005-0011-2

Nork TM, ver Hoeve JN, Poulsen GL, et al., 2000. Swelling and loss of photoreceptors in chronic human and experimental glaucomas. *Arch Ophthalmol*, 118(2):235-245. https://doi.org/10.1001/archopht.118.2.235

Nouri-Mahdavi K, Hoffman D, Coleman AL, et al., 2004. Predictive factors for glaucomatous visual field progression in the advanced glaucoma intervention study. *Ophthalmology*, 111(9):1627-1635. https://doi.org/10.1016/j.ophtha.2004.02.017

Ortín-Martínez A, Salinas-Navarro M, Nadal-Nicolás FM, et al., 2015. Laser-induced ocular hypertension in adult rats does not affect non-RGC neurons in the ganglion cell layer but results in protracted severe loss of cone-photoreceptors. *Exp Eye Res*, 132:17-33. https://doi.org/10.1016/j.exer.2015.01.006

Panda S, Jonas JB, 1992. Decreased photoreceptor count in human eyes with secondary angle-closure glaucoma. *Invest Ophthalmol Vis Sci*, 33(8):2532-2536.

Salminen A, Kauppinen A, Hyttinen JMT, et al., 2010. Endoplasmic reticulum stress in age-related macular degeneration: trigger for neovascularization. *Mol Med*, 16(11-12): 535-542. https://doi.org/10.2119/molmed.2010.00070

Sim D, Fruttiger M, 2013. Keeping blood vessels out of sight. *eLife*, 2:e00948. https://doi.org/10.7554/eLife.00948

Sun H, Wang Y, Pang IH, et al., 2011. Protective effect of a JNK inhibitor against retinal ganglion cell loss induced by acute moderate ocular hypertension. *Mol Vis*, 17: 864-875.

Tham YC, Li X, Wong TY, et al., 2014. Global prevalence of glaucoma and projections of glaucoma burden through 2040: a systematic review and meta-analysis. *Ophthalmology*, 121(11):2081-2090. https://doi.org/10.1016/j.ophtha.2014.05.013

Wang JW, Valiente-Soriano FJ, Nadal-Nicolás FM, et al., 2017. MicroRNA regulation in an animal model of acute ocular hypertension. *Acta Ophthalmol*, 95(1):e10-e21. https://doi.org/10.1111/aos.13227

Weinreb RN, Aung T, Medeiros FA, 2014. The pathophysiology and treatment of glaucoma: a review. *JAMA*, 311(18): 1901-1911. https://doi.org/10.1001/jama.2014.3192

Xu SC, Gauthier AC, Liu J, 2016. The application of a contact lens sensor in detecting 24-hour intraocular pressure-related patterns. *J Ophthalmol*, 2016:4727423. https://doi.org/10.1155/2016/4727423

Xu LJ, Li SL, Zemon V, et al., 2020. Central visual function and inner retinal structure in primary open-angle glaucoma. *J Zhejiang Univ-Sci B (Biomed & Biotechnol)*, 21(4): 305-314. https://doi.org/10.1631/jzus.B1900506.

Yang L, Li SH, Miao LQ, et al., 2016. Rescue of glaucomatous neurodegeneration by differentially modulating neuronal endoplasmic reticulum stress molecules. *J Neurosci*, 36(21):5891-5903. https://doi.org/10.1523/jneurosci.3709-15.2016

Yang LP, Wu LM, Guo XJ, et al., 2007. Activation of endoplasmic reticulum stress in degenerating photoreceptors of the *rd1* mouse. *Invest Ophthalmol Vis Sci*, 48(11):5191-5198. https://doi.org/10.1167/iovs.07-0512

Zeimer RC, Wilensky JT, Gieser DK, et al., 1991. Association between intraocular pressure peaks and progression of visual field loss. *Ophthalmology*, 98(1):64-69. https://doi.org/10.1016/s0161-6420(91)32340-6

Zhao ZN, Yu XW, Yang X, et al., 2020. Elevated intraocular pressure causes cellular and molecular retinal injuries, advocating a more moderate intraocular pressure setting during phacoemulsification surgery. *Int Ophthalmol*, 40(12): 3323-3336. https://doi.org/10.1007/s10792-020-01519-w

Zhou L, Chen W, Lin DY, et al., 2019. Neuronal apoptosis, axon damage and synapse loss occur synchronously in acute ocular hypertension. *Exp Eye Res*, 180:77-85. https://doi.org/10.1016/j.exer.2018.12.006

Supplementary information

Table S1